Thermal and kinetic analysis of diverse biomass fuels under different reaction environment: A way forward to renewable energy sources

Farooq Sher[a,*], Sania Z. Iqbal[b], Hao Liu[c], Muhammad Imran[d], Colin E. Snape[c]

a. School of Mechanical, Aerospace and Automotive Engineering, Coventry University, Coventry CV1 2JH, UK

b. Department of Biochemistry, University of Agriculture, Faisalabad, 38000, Pakistan

c. Faculty of Engineering, University of Nottingham, University Park, Nottingham NG7 2RD, UK

d. School of Engineering and Applied Science, Aston University, Aston Triangle, Birmingham B4 7ET, UK

*Corresponding author:

Dr F. Sher
Lecturer
School of Mechanical, Aerospace and Automotive Engineering
Faculty of Engineering, Environmental and Computing
Coventry University
Coventry
CV1 2JH
UK

E-mail address: Farooq.Sher@coventry.ac.uk (F.Sher)
Tel.: +44 (0) 24 7765 7754, Fax: +44 (0) 24 7765 7754

Abstract

This study investigates the thermal and kinetic analysis of six diverse biomass fuels, in order to provide valuable information for power and energy generation. Pyrolytic, combustion and kinetic analyses of barley straw, miscanthus, waste wood, wheat straw, short rotation coppicing (SRC) willow and wood pellet were examined by non-isothermal thermogravimetry analyser (TGA), differential thermogravimetric (DTG) and differential scanning calorimetry (DSC) techniques. Biomass fuels were thermally degraded under N_2, air, CO_2 and the selected oxy-fuel (30% O_2/ 70% CO_2) reaction environments. The thermal degradation under inert N_2 and CO_2 atmospheres showed an almost identical rate of weight loss (R), reactivity ($R_M \times 10^3$) and activation energy (E_a) profiles. Similar profiles for R, R_M and E_a were observed for the environments under air (21% O_2/ 79% N_2) and the oxy-fuel combustion. Results indicated that the thermal decomposition rate for biomass fuels in an oxidising condition was faster than in an inert atmosphere, favourable effect on thermal degradation of biomass fuels was observed when oxygen content increased from 21 to 30%. Higher activation energies with lower reactivity were observed for the biomass fuels that have low cellulosic contents as compared to the other fuels. Regression analysis confirmed that the reaction order 0.5 modelled fitted well for all biomass samples. All these findings will provide valuable information and promote the advancement of future researches in this field.

Keywords: Renewable energy; Biomass; Oxy-fuel combustion; Activation energy, Heat flow kinetics and Carbon emissions.

1. Introduction

There is a crucial requisite of global alteration from coal energy to renewable bio-energy sources [1]. As carbon-negative and renewable origin of bio-energy, biomass fuels can play a chief role. Biomass energy, a form of solar energy stored in plant matter, is considered to be environmental friendly and carbon-neutral if the consumption and growth of the biomass are kept in balance. When CO_2 emissions produced from biomass utilisation is captured and stored, negative carbon emissions can be achieved. Biomass fuels are also often regarded as the cleaner fuel for power generation as they tend to have appreciably lower sulphur contents than fossil fuels [2]. Furthermore, biomass fuels can be used to deliver controllable energy that is free from the problem of intermittency which is inherent with the wind and solar energies.

Therefore, biomasses are the potential major future renewable energy resources, with developed bio-energy systems being considered as vital contributors to future sustainable energy production [3, 4]. Pyrolysis is an important fundamental process that can be used to study the thermochemical conversion of biomasses into the biomass char and gaseous or liquid fuels [5]. It is also used to improve gasification, fixed carbon content, calorific value and combustion processes. The combustion process is of great significance in boilers and furnaces, that's why a sound knowledge of this process is required to determine the feasibility of the biomass fuel [6, 7]. In addition, kinetic study is considered as an important criteria for the measurement of reactivity and combustibility potentials of the biomass fuels. Pyrolytic and combustion characteristics of the biomass fuels have been studied mostly with thermogravimetric analyser (TGA) in literature with a focus on a range of working reactant environment for thermal degradation [8]. TGA has also been used to identify different polymeric lignocellulosic fractions present in biomass residues and to determine the reactivities of char residues in the presence of active atmospheres of interest [9].

The kinetic parameters derived from TGA analysis are used to design combustors, pyrolysis reactors and gasifiers. Mansaray and Ghaly [10], investigated the thermal decomposition profile of four rice husk selections using TGA, under N_2 at three different heating rates. Direct increase in thermal degradation with increasing heat rates was observed in their research. On the other hand, lower the cellulosic amount of the biomass, the lower the temperature noted for its decomposition. Moreover, the greater the cellulose amount the greater thermal degradation rate and the higher the initial degradation temperatures. Munir et al. [11] studied non-isothermal degradation and devolatilisation kinetics of four biomass fuels including shea meal, two different sugarcane bagasse residues and cotton stalk under an inert N_2 and oxidising (21% O_2/ 79% N_2) environment conditions. They found that the cotton stalk was the reactive biomass in comparison to other, under both environments, whereas Shea meal was the least reactive biomass in inert environment because of its low amount of volatile matter and low oxygen to carbon ratio value. However, the generation of complex char under oxidant combustion by Shea meal was indicative of different types of char resulting from fibrous and woody constituents in the original biomass.

When the reaction gas environment is CO_2 [12] or oxy-fuel combustion which is mainly composed of O_2 and CO_2. The CO_2-char gasification reaction has been studied by various researchers [13-17] is a chief reaction in the biomass thermal decomposition, especially in the high temperature zone. The most important CO_2-char gasification reaction is the Boudouad reaction Eq. (1):

$$C + CO_2 \leftrightarrow 2CO \quad (1)$$

Where C represents the active site of reaction and C(O) represent complex formation between carbon and oxygen. The carbon monoxide (CO) presence generates a constraining influence

by dropping the C(O) steady state amount. Different studies [13, 18-20] about pyrolysis and combustion of coal and/or biomass blends using thermogravimetric analysis are available, but few have examined the effects of different gas mixtures, especially oxy-fuel gases on the thermochemical 100% conversions of biomasses especially non-woody biomass fuels.

In order to provide valuable information for biomass fuel in the UK for power and energy generation, this study investigated the thermal and kinetic behaviour of different local biomasses. Biomass fuels thermally degraded in different atmospheric conditions such as CO_2, N_2, air and oxy-fuel (30% O_2/ 70% CO_2). Pyrolysis and combustion analyses were performed. Impact of reactant gas mixtures on biomass fuels' reactivity parameters (reaction rate constants, rate of weight loss, peak temperature, activation energy etc.) was measured by TGA, differential thermogravimetry (DTG), differential scanning calorimetry (DSC) and Arrhenius equation. In addition to all these, quantitative assessment of polymeric lignocellulosic components of biomasses was also examined using DTG plots of biomasses. Previously researchers examined the thermal characteristics of the fuels using just one or in the rare case under two experimental conditions, while herein the biomass samples were examined under four different reaction conditions (N_2, oxy-fuel, CO_2 and air) ranges from inert to highly oxidant, for the identification of best fuels for the UK's energy demands. A detail kinetic study of the biomass fuels was carried out by the calculation of reactivity, activation energy, heat flow and mass transfer rates.

2. Experimental

2.1 Materials and sample preparation

Six different biomass fuel samples were used: barley straw (BS), miscanthus (MIS), waste wood (WD), wheat straw (WS), willow SRC (SRC) and wood pellet (WP). The biomass fuels

were obtained as pellets from different suppliers in the UK. These fuels were produced and processed in the UK. The wood pellet was a commercial product "Brites" from Balcas Ltd and commercially used in domestic boilers, while the other biomass pellets were produced by the suppliers as potential alternative biomass fuels for commercial use. Before analysis, all fuel samples were ground to size ≤212 μm using a Retsch ultra centrifugal mill ZM 200 as the relevant analytical standards require the particle size ≤212 μm [21]. The fuel samples were ground to the same particle size to elude their effects on thermal degradation [6].

2.2 Fuel analyses

Flash EA 1112 elemental analyser and TA Instruments TGA Q-500 thermogravimetric analyser were used for ultimate and proximate analysis respectively. Proximate analysis was obtained by heating the sample under N_2 at a rate of 10 ^oC/min and temperature 110 ^oC. To get the moisture content maintained these condition for up to 10 min. The temperature was then increased from 110 to 700 ^oC and the heating rate increased from 10 to 20 ^oC/min. Set these conditions for half an hour to get the weight loss by devolatilisation after this the temperature was ramped at the same rate 20 ^oC/min to 950 ^oC. After that, the reaction environment was changed from N_2 to air inside the furnace chamber and kept it isothermal for 40 min to oxidise the char completely to obtain the fixed carbon and ash contents [22]. Channiwala and Parikh (2002) suggested Eq. (2), was used for calculating the high heating value (HHV) of each selected sample, which gives 1.45% absolute error and 0.00% bias error [23].

$$HHV = 0.3491C+1.1783H+0.105S–0.1034O–0.0151N–0.0211A \quad (2)$$

The HHV value is also dependent on ash (A) contents of biomasses. The elemental and proximate analyses along with high heating values (HHV) for these samples are represented in Table 1 along with the results reported elsewhere. The overall analysis shows that all biomass samples have lower moisture content < 8.9%, and high volatiles and oxygen contents. On the

other hand, their nitrogen contents are low (0.07–2%). It is also noticed that these samples have sulphur contents 0.00%, below the detection limit. All the biomass fuel samples contain moisture < 8.9%. Therefore, it is verified in correlation from literature, that these samples could become the good fuels for the UK power industry. It is reported that biomass having moisture content < 10 % is considered a good fuel for pyrolysis and combustion [2].

The amount of elemental and proximate content of the studied biomass fuel samples are compared with other biomasses [18], coal [18] and lignite (low rank coal) [24]. The carbon content of biomass samples ranges (40.87–47.02%). The C content (Table 1) values of BS, MIS and WS are comparable with others while those of SRC, WW and WP are higher than the reported biomasses (40.93–43.19%) and lignite (44.82%). Wheat straw (WS) contains the highest fixed carbon at 18.22%, whereas, SRC has the highest amount of volatile matter at 85%. Biomass HHV's vary from 15.46 to 18.83 MJ/ kg. The higher C and H content and lower O content of wood pellet (WP) in comparison with other samples, results in higher calorific value. It has been described that HHVs increase with an increase in cellulosic content of the biomass fuel, correlate with the polymeric lignocellulosic analysis of these samples as well [25].

Table 1. Ultimate, proximate analysis and calorific values of biomass and other fuels.

Fuels	Ultimate analysis[a]					Proximate analysis[c]				HHV[d] (MJ/kg)
	C (%)	H (%)	N (%)	O[b] (%)	S (%)	M (%)	VM (%)	FC (%)	Ash (%)	
Barley straw (BS)	40.87	5.78	0.55	52.80	0.00	8.95	78.15	14.70	7.15	15.46
Miscanthus (MIS)	42.67	5.86	0.44	51.04	0.00	6.91	78.29	16.33	5.38	16.40
Waste wood (WW)	45.78	6.05	0.34	47.84	0.00	5.80	84.48	14.06	1.46	18.12
Wheat straw (WS)	41.32	5.69	1.18	51.81	0.00	6.41	72.28	18.22	9.50	15.56
Willow SRC (SRC)	45.18	5.99	0.32	48.51	0.00	5.97	85.00	13.24	1.77	17.77
Wood pellet (WP)	47.02	6.17	0.07	46.75	0.00	6.34	84.94	14.28	0.79	18.83
EFB [18]	40.93	5.42	1.56	51.78	0.31	----	70.5	15.4	4.5	16.8
PMF [18]	43.19	5.24	1.59	49.79	0.19	----	68.8	15.2	10.2	19.0
Lignite [24] (brown coal)	44.82	2.98	0.81	50.21	1.60	----	----	----	----	16.38
Coal [18]	54.37	5.29	1.75	38.34	0.25	----	42.2	48.8	5.8	24.6

M: moisture, VM: volatile matter, FC: fixed carbon, HHV: high heating value, EFB: empty fruit bunches, PMF: mesocarp fibre

a. On dry basis except as denoted in the table.
b. Calculated by the difference.
c. On dry basis except moisture which is on as received basis.
d. Calculated based on Channiwala and Parikh [23].

2.3 Experimental techniques and kinetic analysis

The pyrolysis and combustion or gasification kinetics of all fuels were studied under dynamic conditions in N_2, air (21% O_2/ 79% N_2), CO_2 and a typical oxy-fuel (30% O_2/70% CO_2), using a non-isothermal conditioned TGA. This method has distinct benefits over the classic isothermal TGA. Firstly, this analysis reduces the thermal induction period errors; secondly, it allows a rapid scan over the desired whole range of temperature. Therefore, many researches have opted the non-isothermal TGA to study pyrolysis of many solid fuels [26, 27].

The weight of each sample was limited to 15–20 mg for each TGA test, to avoid the potential effect of heat flow and mass conversion. For each TGA test, first the temperature was ramped from ambient to 110 ^oC at 10 ^oC/min heating rate and maintained these conditions for 10 min. Then it was increased at 20 ^oC/min to 950 ^oC and held for 40 min. A 100 mL/min constant rate of gas flow was applied for all gas conditions. Weight loss profiles and their derivative curves

193 (differential thermogravimetry–DTG) were then obtained as a function of time and temperature
194 for the reaction conditions examined.

195 ***2.3.1. Error analysis***

196 Between three and four repeat runs for each biomass fuel were performed to ensure appropriate
197 repeatability and statistical validity of the results. The average difference between the repeated
198 runs was <2% for all type of fuels. Mainly three sources are responsible for errors in TGA
199 measurements: (a) TGA instrument, (b) minor fluctuation in sample's weight measurements
200 by operator, and (c) environmental interference. Standard materials/chemicals with known
201 melting points were used to minimise the effects of TGA instrument errors. In addition to this,
202 TGA-instrument was preheated for 60 min to homogenise the environment before
203 measurements were carried out. An electronic weight balance, was used to minimize the
204 operator's error, having a maximum weighing capacity of 60 g with 0.1 mg lower readability
205 efficiency [28].

206

207 ***2.3.2. Kinetic analysis***

208 Several methods are available for determining the kinetics of non-isothermal thermolysis.
209 However, the method used in this research for the determination of activation energy was based
210 on the Arrhenius equation [13, 29]. This has been found to yield acceptable results by a number
211 of researchers [13, 30]. The formulas used to calculate the decomposition reaction kinetics are
212 as follows:

213 $$\frac{\mathrm{dx}}{\mathrm{dt}} = k\mathrm{f(x)} \qquad (3)$$

214 where k is the rate constant, x is the conversion rate, t is time, $f(x) = (1-x)^n$ and n is the order
215 of reaction.

216 According to the Arrhenius correlation, the rate constant is described as:

217 $$\mathrm{k} = \mathrm{A}\exp\left(-\frac{\mathrm{E_a}}{\mathrm{RT}}\right) \qquad (4)$$

Where A is the pre-exponential factor, E_a is the activation energy, R the universal gas constant and T the reaction temperature. Thus, combining Eq. (3) and Eq. (4) gives:

$$\frac{dx}{dt} = A\exp\left(-\frac{E_a}{RT}\right)(1-x)^n \quad (5)$$

Incorporating the non-isothermal TGA heating rate, β=dT/dt in Eq. (5) gives:

$$\frac{dx}{dt} = \left(\frac{A}{\beta}\right)\exp\left(-\frac{E_a}{RT}\right)(1-x)^n \quad (6)$$

Taking natural logarithm of both sides of Eq. (6) yields:

$$\ln\left[\left(\frac{dx}{dT}\right)(1-x)^n\right] = \ln\left[\frac{A}{\beta}\right] - \frac{E_a}{RT} \quad (7)$$

According to Eq. (7), a plot of ln $[(dx/dT)/(1-x)^n]$ versus 1/T should yield a straight line with a slope of $(-E_a/R)$ for different values of n resulting in a regression coefficient near to unity. Eq. (7) was used to obtain kinetic parameters for each experiment.

TGA and DTG profiles guide about the biomass fuels thermal stability and the overall kinetic decomposition. Both these profiles were used to identify other combustion characteristics including average rate of weight loss (R_{avg}), average temperature (T_{avg}), peak temperature (T_{peak}) and maximum rate of weight loss (R_{max}) for all studied biomass fuels [11, 31]. T_{peak} corresponds to the point at which the reaction is proceeding at its maximum rate, and R_{max} is the associated weight loss rate at T_{peak}. The selection of viable temperature ranges for analysing devolatilisation and combustion reactions can have a significant impact on the calculated values. However, there is no general consensus on which approach is the best [32, 33]. In this

study, a formulation originally devised by Ghetti et al. [34] represented in Eq. (8) has been employed to calculate the reactivities of the biomass fuel samples:

$$R_M \times 100 = \frac{R_{M1}}{T_{P1}} + \frac{R_{M2}}{T_{P2}} + \frac{R_{M3}}{T_{P3}} \ldots\ldots\ldots + \frac{R_{Mn}}{T_{Pn}} \quad (8)$$

Where R_M and T_P is the factor of mean reactivity, height of DTG peak and corresponding peak temperature, respectively.

To more closely study the kinetics, heat flow profiles of the biomass fuels differential scanning calorimetry (DSC) technique under N_2 and air reaction environments was performed. The DSC analysis was performed by SDT TA Q600 instrument at 20 ^oC/min heating rate. DSC analyses were performed to detect the endo and exothermic nature of the reactions, as heat transfer during pyrolysis and combustion process [35]. Furthermore, the mass transfer rate of biomass fuels were calculated by using the method of Pottmaier et al. [35].

3. Results and discussion

3.1 Van Krevelen Diagram

The biomass samples are compared with other solid hydrocarbon fuels in Fig. S1 using the Van Krevelen diagram, a cross plot diagram of H: C as a function of O: C. Devised by Dirk Willem van Krevelen, the diagram permits a better understanding of the evolution path of organic matter/ rank and is indicative of different regions associated with solid fuels. As can be seen from Fig. S1, the biomass samples studied are localised in the region typically associated with biomass. However, they were seen to be relatively uniform in their H/C ratio but varying by 30% in their O/C ratios from WP at 0.99 to BS at 1.29.

This likely evidences the higher proportion of mineral oxides present in straw and grass species (Family: *Poacae)*, known to be effective gasification catalysts [36], but with a propensity to melt and sinter in the high temperatures of reactors, causing fused deposits [37]. In general, various types of coal fuels are limited in the range of $0 \leq H/C \leq 0.1$ and $0 \leq O/C \leq 0.3$ whereas biomass fuels having a higher proportion of O/H are categorised in the limits of $0.7 \leq O/C \leq 1.3$ and $0.075 \leq H/C \leq 0.25$.

3.2 Thermal degradation under N_2 atmosphere

Fig. 1a shows the weight loss profiles of the selected biomass fuels during the non-isothermal TGA tests under N_2. It is well known that cellulose, hemicellulose and lignin are the major natural polymeric components of the biomass fuels. But different kinds of biomass contain varying types and proportions of cellulose, hemicellulose, lignin and a small amount of other extractives. The thermal decomposition of the main organic components of the biomass generates oxygenated by-products. As the temperature gradually increases, these by-products reach their spontaneous ignition and the released heat contributes to the decomposition of the remaining organic matter [11]. Such behaviour can also be observed in Fig. 1a by means of a continuous mass loss due to the slight devolatilisation up to the end of the heating programming. The weight loss (wt% /min) of 7, 6.4, 4.8, 6, 5.3 and 5.1% occurred between 25 and 110 °C for BS, MIS, WW, WS, SRC and WP respectively. This initial weight loss (< 110 °C) is associated with moisture evolution. Devitalization of BS, MIS, WW, WS, SRC and WP is initiated at different corresponding temperatures of 190, 205, 210, 195, 215 and 220 °C respectively. This variation in devolatilisation temperatures could be related to different elemental and chemical compositions of these biomass fuels [38].

Quantitative assessment of polymeric components of biomasses was examined using differential thermogravimetric (DTG) plots of biomasses under N_2. Pyrolysis of biomass under

289 inert atmosphere can be divided into three stages; first moisture evolution, then devolatilisation
290 and finally continuous slight devolatilisation [39]. The DTG plots of biomasses under N_2 are
291 represented in Fig. 1b. It is difficult to clearly distinguish between hemicellulose and cellulose
292 devolatilisation regions for WW in contrast to other fuels (i.e. SRC; BS; MIS). This is due to
293 the inhomogeneous nature of this mixed original woody-biomass sample. At the end of the
294 major peak the slow degradation over a wider temperature range continues to produce pyrolysis
295 residue reaching to a constant ratio, sometimes referred to as long tailing section [11, 39]. The
296 maximum rates of weight loss (wt% /min) were 16, 17.4, 17.7, 14.9, 19.3 and 19% for BS,
297 MIS, WW, WS, SRC and WP respectively. These weight loss rates were found to be higher
298 for the fuels with higher volatile matter and lower ash contents [11]. The thermal degradation
299 results under N_2 are presented in Table S1.
300

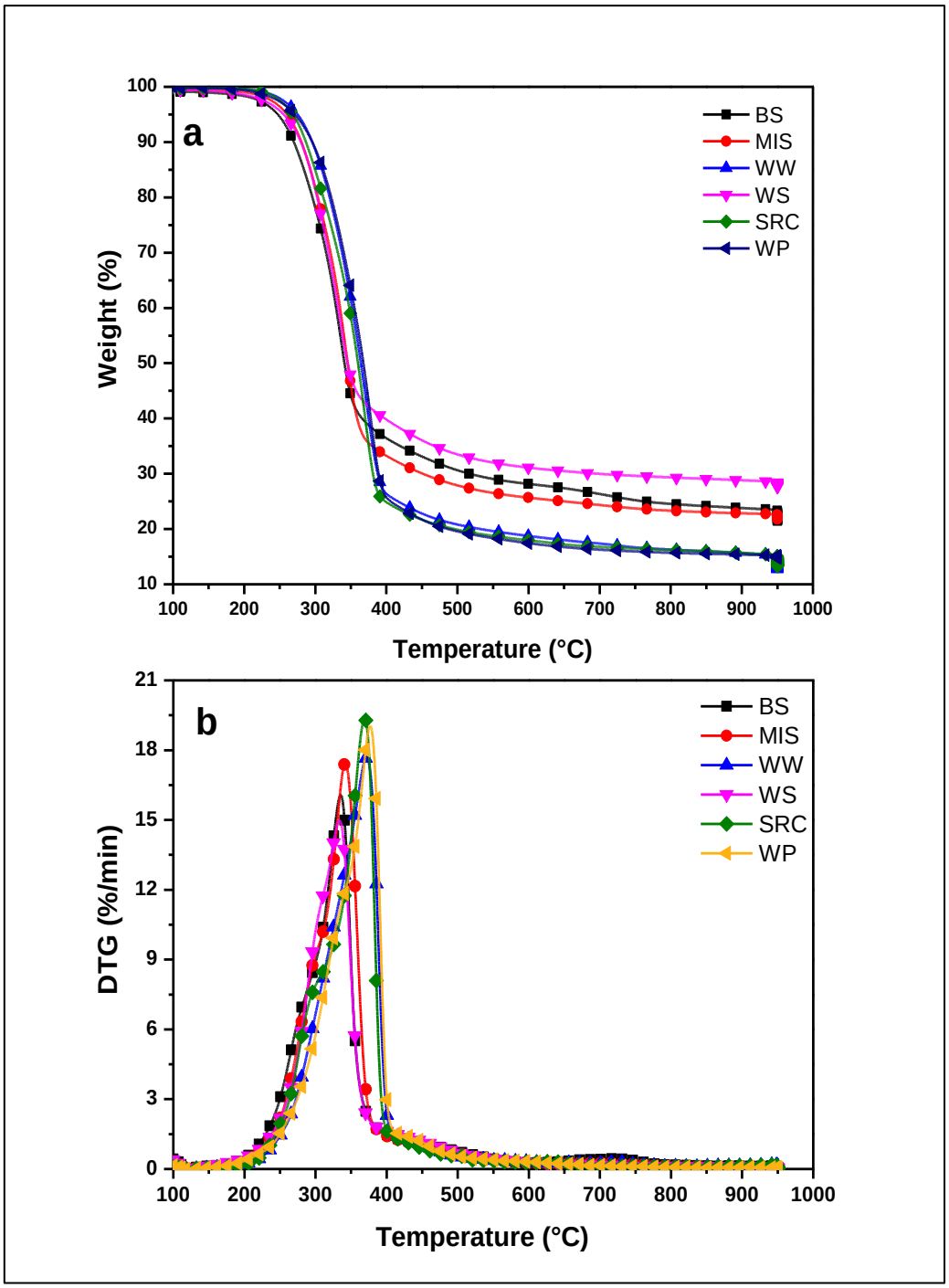

Fig. 1. Thermal degradation profiles of biomass fuels under N_2 atmosphere: (a) TGA curves, (b) DTG curves.

Usually, biomass fuels having high cellulose contents are recommendable for bio-thermal conversion processes, whereas those with high lignin contents are particularly suitable for combustion and/or gasification applications. The devolatilisation rate of the lignocellulosic biomass under nitrogen atmosphere depends on number of other components such as higher

the lignin content, the slower the biomass devolatilisation [40]. The temperature range of lignin devolatilisation cannot be discerned from, which often has a broad peak temperature overlapping that of cellulose decomposition [41]. It is evaluated and reported [42], that DTG method gives comparable results than the other available common methods (holocellulose extraction, cellulose extraction, neutral detergent fibre, acid detergent fibre and acid detergent lignin). All experimentations were performed side by side for comparison. Moreover, the DTG method is cost effective, easier to implement and faster than the above mentioned wet chemical analyses. Therefore, in this study hemicellulose and cellulose contents of biomass fuels are calculated from DTG curves using a method shown in Fig. 2 and presented in Table 2, along with those reported elsewhere.

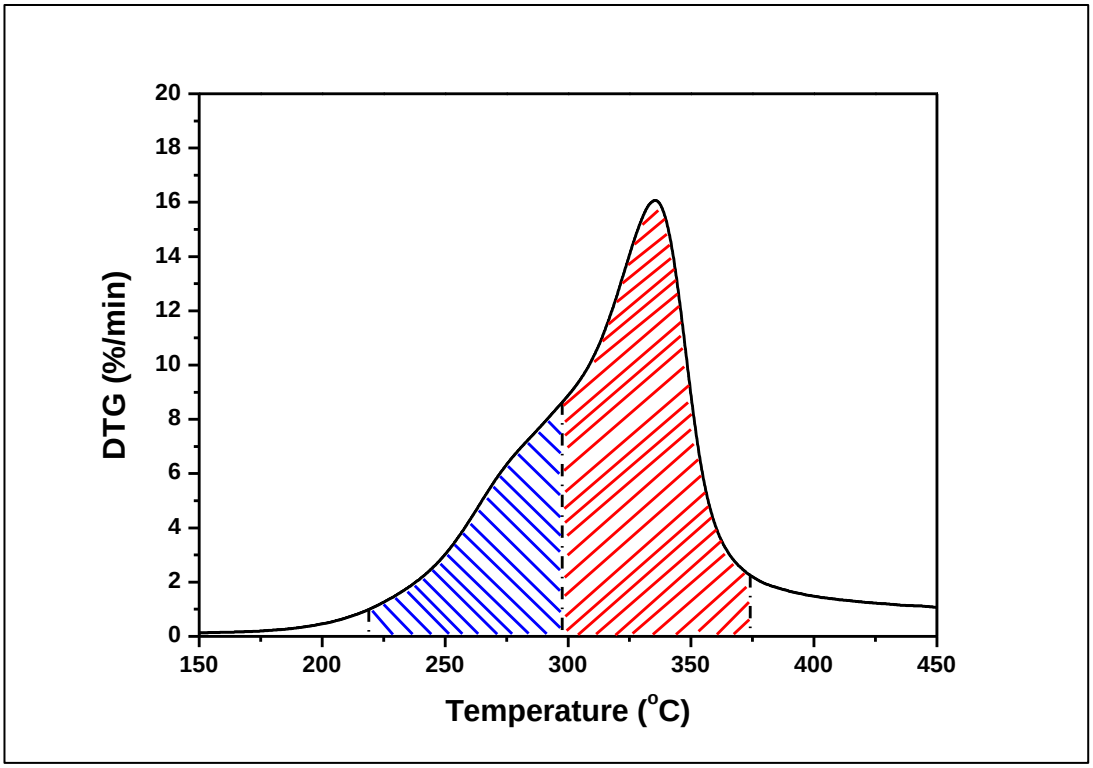

Fig. 2. Typical DTG profile for a biomass fuel under N_2, weight loss under the first shoulder (shaded blue) in the first DTG peak corresponds to hemicellulose contents and the weight loss under the main DTG peak (shaded red) corresponds to cellulose contents.

The criteria for division of area under the DTG curve was the observed two shoulders. The DTG plot in Fig. 2 shows the apparent two-stage (two shoulders) release of the first hemicellulose (low temperature) and then cellulose (high temperature). This temperature dependent release of cellulosic components is in accordance with the literature [42]. Weight loss under the first shoulder (shaded blue) in the first DTG peak corresponds to hemicellulose contents and the weight loss under the main DTG peak (shaded red) corresponds to cellulose contents. Due to the difficulties to measure lignin content, an error of +/- 11% can be attributed to this study's results as compared with other published results.

Table 2. Compositions of main lignocellulosic components in different biomass fuels.

Fuels (from this study unless stated)	**Cellulose (**wt%)	**Hemicellulose** (wt%)	**Lignin** (wt%)	**Reference**
BS*	40.00	20.00	-	This study
MIS*	40.00	21.00	-	This study
WS*	35.00	20.00	-	This study
SRC*	60.00	12.00	-	This study
WP*	38.00	30.00	-	This study
WS	33–45	20–32	8–20	[43]
	41.30	30.80	7.70	[44]
SRC	49.3	14.10	20	[44]
BS	33.3–42	20.4–28.0	17.10	[43]
MIS	40.0	18.0	25.0	[43]
	38.8	36.6	11.5	[45]

*****Anticipated wt% loss attributed to hemicellulose and cellulose calculated from DTG.

While the comparison with other studies [44, 46-49] based on a common method for determination of polymeric lignocellulosic components, it is proved that the values predicted by using present DTG technique were comparable. Previous studies on biomass have shown that cellulose comprises 40–50% compared to 20–40% of hemicellulose and 10–40% lignin [50]. The relative proportions of cellulose and lignin are two of the determining factors in

identifying the suitability of biomass fuels for the energy production process since the ratio of cellulose to lignin dictates the rates of thermal decomposition [40]. The final pyrolysis residues were in the range of 14.3 to 21.7% that comprised of unburnt char and ash.

3.3 Thermal degradation under air atmosphere

As shown in Fig. 3a and b, most of the biomass fuels demonstrated three-stage weight loss under oxidative environments: the first stage of moisture evaluation, the second for oxidative degradation and the third relates to char combustion. The TGA and DTG profiles obtained under air were different from those under N_2, showing elevated reaction rates in the air. The DTG peaks under air are shown in Fig. 3b, different peaks and mass loss stages are attributable to moisture evolution and devolatilisation occurred; but with devolatilisation, higher global reaction rates are apparent, evidencing the predominance of different decomposition pathways. The peaks between 215 to 370 ^{o}C are attributed to the devolatilisation zone. In the first zone, BS started to react earliest from 205 ^{o}C with a weight loss of 53%, whereas WP started last from 235 ^{o}C with the highest weight loss of 63% (see Fig. 3a).

The thermal degradation results in the first and second reaction zones under air are summarized in Table S1. The maximum rate of weight loss (R_{max}) of 39.7% at the peak temperatures (T_{peak}) of 288 ^{o}C was observed for BS. Devolatilisation under air was occurred at a lower temperature than under N_2. The average rate of weight loss (R_{avg}) were 10.3, 11, 9.4, 9.4, 10.2 and 9.3% for BS, MIS, WW, WS, SRC and WP respectively. These values are almost twice than under N_2, also supported by previous research [11]. Higher decomposition rates within a narrow temperature range are also observed in this region which is associated with cellulose chemical decomposition [40]. After devolatilisation, char combustion begins. An apparent overlapping between these two zones is observed, over temperature periods of 80, 45, 38, 20, 48 and 40 ^{o}C for BS, MIS, WW, WS, SRC and WP respectively. It had previously been reported [51] that

366 char oxidation could be started during devolatilisation if oxygen reaches the particle's surface.
367 The mass loss that was observed to occur over a broad range, relatively higher temperature
368 region marked as region A in Fig. 3b, between 385 to 540 ^{o}C. This is believed to correspond
369 to the char combustion zone. The anticipated char (also have ash) contents of 22.5, 23.5, 30,
370 19.5 and 24% attributed between temperature regions 360–460, 390–510, 340–570, 410–510
371 and 410–540 ^{o}C for MIS, WW, WS, SRC and WP respectively.

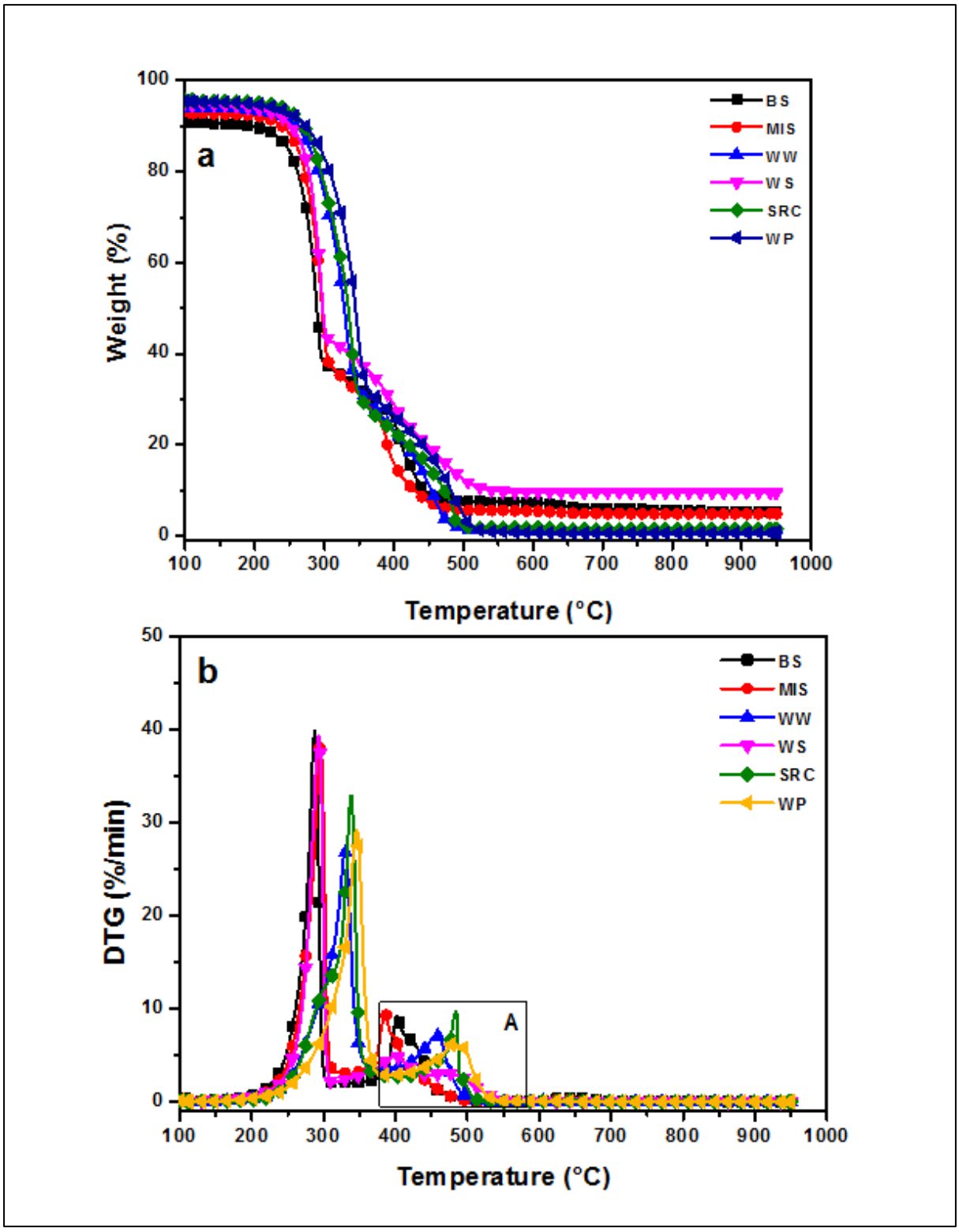

372

373 **Fig. 3.** Thermal degradation profiles of biomass fuels under air: (a) TGA curves, (b) DTG curves.

374

375 The rate of reaction for all type of biomass fuels during combustion becomes faster than that

376 of pyrolysis and devolatilisation. The maximum rate of weight loss during char combustion

was found to be 9.47% for SRC. The SRC rate of weight loss during combustion is the highest among all other fuels with the highest cellulose contents about 60%. The cellulose content in the biomass may enhance the ignition characteristics and decomposition process of lignin since cellulose compounds have a branching chain of polysaccharides rather than an aromatic ring, which are easily volatilised.

The residue left at the end of the combustion actually comprises of ash. A wide variation in the ash content can be observed within non-woody biomass fuels and between other types. Irrigation and fertilizer usage in the growth of herbaceous plants leads to higher contents for almost every inorganic species in comparison to wood. The highest ash content of 9.4% is found with WS. The alkali content is much higher in non-woody biomasses (herbaceous materials) in comparison with woody biomasses. In general, silica and potassium are the two major ash forming species for all of the agricultural biomass fuels [52].

3.4 Thermal degradation under CO_2 atmosphere

The thermal behaviour of biomass fuels under CO_2 is shown in Fig. 4. It is evident from Fig. 1a, that when N_2 is used, the end point of devolatilisation cannot be found after the residence time of the isotherm condition. On the other hand, the use of CO_2 (Fig. 4a) highly improves the trend towards reaching a mass loss plateau in the isothermal step and enables the distinction and quantification of the volatile material and fixed carbon contents in biomass samples. According to Borrego and Alvarez [53], the use of CO_2 as a carrier gas provides higher resistance to the devolatilisation of bulk components of biomass in relation to N_2. This resistance may be due to the involvement of CO_2 in the cross-linking reaction on the char surface, which reduces the deformation and clumps its carbonaceous structure.

401 The onset of devolatilisation was seen to occur at higher temperatures in the presence of CO_2
402 compared to N_2 which is shown in Fig. 4b. The average temperatures for devolatilisation
403 region being higher under CO_2 flow than N_2 (Table 4). The difference in the values of specific
404 heat capacity and thermal conductivity for CO_2 and N_2 influences the degradation/ combustion
405 characteristics of the fuels. It has been found that combustion temperatures are substantially
406 affected by replacement of N_2 with CO_2 with/ without the presence of oxygen [54, 55]. Thus,
407 replacing N_2 with CO_2 would adversely effects the energy input required for biomass
408 combustion applications.
409
410 The third peak shown in Fig. 4b after devolatilisation at higher temperatures (>700 ^oC signifies
411 the gasification of pyrolysis char via the Bouduard reaction [31]. As illustrated in Eq. (9), at
412 lower temperatures (< 700 ^oC), less stable compounds are released and char is formed by the
413 devolatilisation process shown in Eq. (9).
414
415

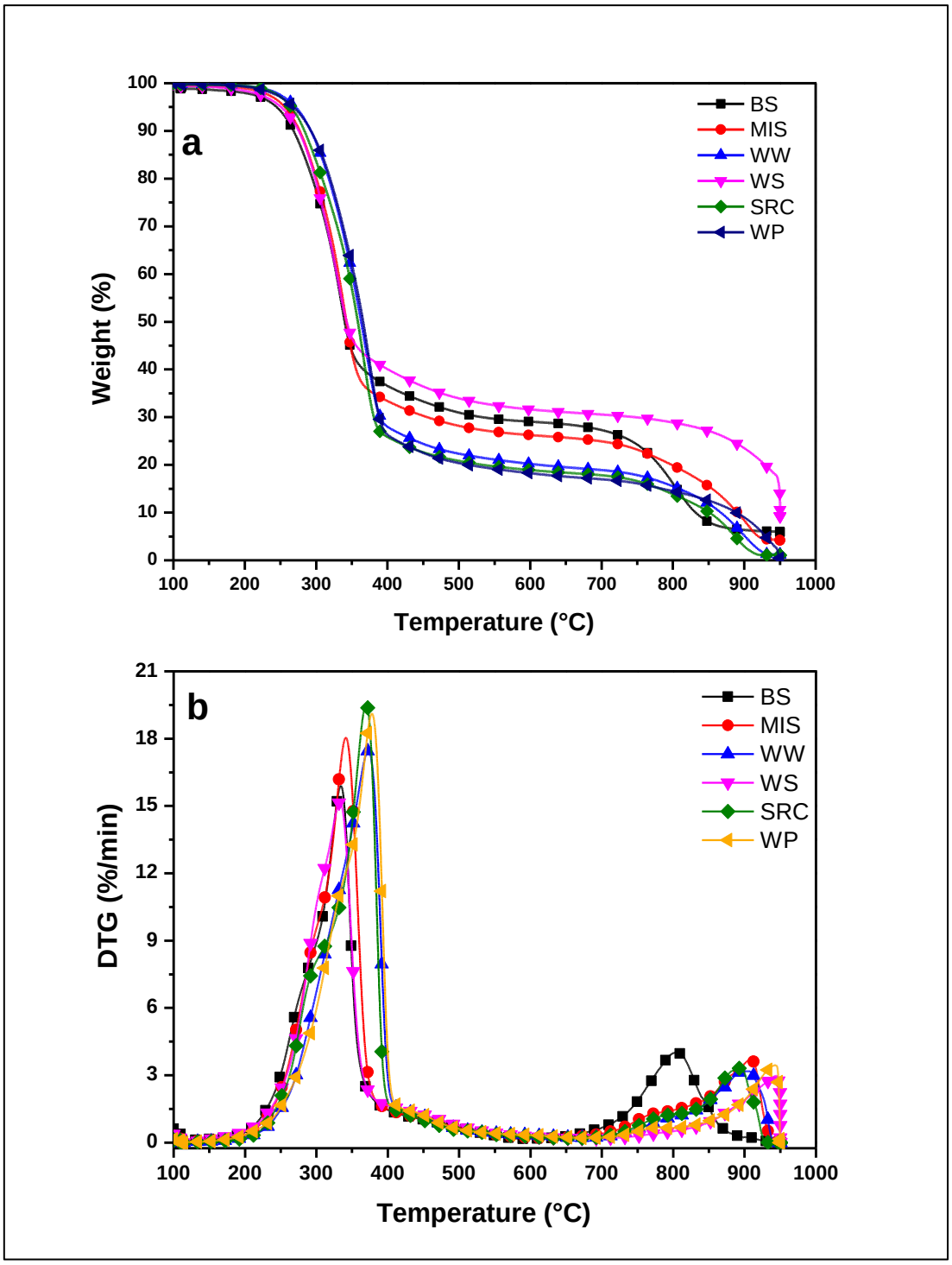

Fig. 4. Thermal degradation profiles of biomass fuels under CO_2: (a) TGA curves, (b) DTG curve.

The char in contact with CO_2 at higher temperatures (> 700 °C) and with enough residence time may undergo a Boudouard reaction, which leads to CO formation [56].

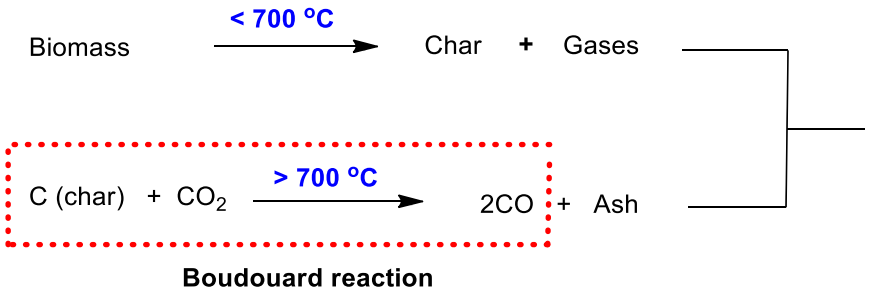

(9)

Higher peak temperatures for char gasification under CO_2 reaction atmosphere are indicative of possible delayed combustion as compared to combustion in air.

3.5 Thermal degradation under the oxy-fuel combustion condition

Recently one of the most studied CO_2 capture and storage technology is oxy-fuel combustion, It is considered as technically feasible to capture up to 95% of pure CO_2 much higher than pure CO_2 production from air combustion, and practically ready for sequestration [57]. Mass losses of all tested biomass fuel samples under the oxy-fuel combustion condition (30% O_2/70% CO_2) are shown in Fig. 5 that are somewhat different from those of air combustion shown as in Fig. 3. In devolatilisation zone WS starting earlier at temperature 210 °C, but BS was the earliest fuel under air; while WP starting later at temperature 230 °C was similar to the air run but at 235 °C. The DTG profiles in Fig. 5b show the biomass fuels decompose with high decomposition rates in rather small temperature intervals. The biomass fuels with high cellulose contents such as BS, MIS, and SRC produce sharp DTG peaks with a small amount of char residue.

The differences in initial degradation temperatures in the first zone (devolatilisation) were 5.0 °C for BS, 18 °C for MIS, 12 °C for WW and 8 °C for SRC. The total weight losses during devolatilisation were in the range of 52 to 70% for all studied biomass fuels; 53% for BS, 58% for MIS, 62% for WW, 52% for WS, 70% for SRC and 66% for WP. Among all the studied

443 fuels, the maximum rate of weight loss (R_{max}); lowest 28% for WW and the highest 47.4% for
444 MIS were observed in the first reaction zone. These weight losses were slightly higher than
445 under air condition (except BS and WW), e.g. 2.5% for MIS, 0.5% for WS, 3.5% for SRC and
446 3% for WP. The difference in the degradation temperatures and rate of weight loss is due to
447 the difference in cellulose, hemicellulose and lignin contents of biomass samples; this fact is
448 extensively reported in the literature [58].

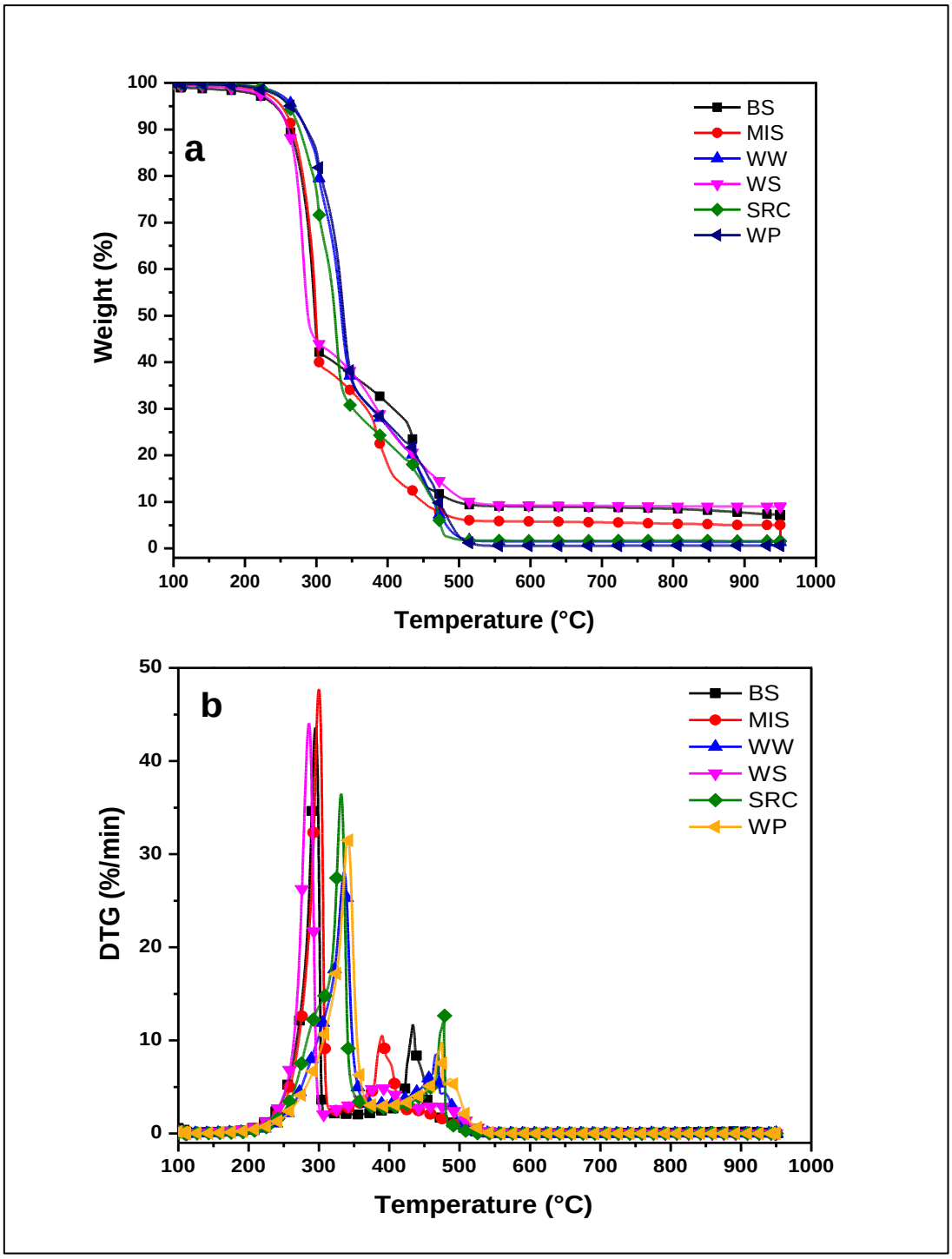

449

450 **Fig. 5.** Thermal degradation profiles of biomass fuels under oxy-fuel environment: (a) TGA curves,
451 (b) DTG curves.

452

453 Similar overlapping zone as under air was observed, but with higher temperature ranges. The
454 anticipated overlapping temperature ranges were found as 95, 55, 50, 25, 80 and 65 °C for BS,
455 MIS, WW, WS, SRC and WP respectively. This higher degree overlapping may be attributed

456 to higher oxygen contents in oxidising gas as compared to air. It is also supported by the
457 literature that char combustion time increases in relation to the pyrolysis under low oxygen
458 contents and relative time of overlapping reduces as under air [51]. The second weight loss
459 zone is attributed with char combustion within the temperature range of 315–535 °C. Similarly,
460 as in the first reaction zone, WS char combustion is taking place before all the other fuels at
461 315 °C and WP on the end at 435 °C. The differences in the temperatures of the second reaction
462 zone were 97 °C for BS, 53 °C for MIS, 100 °C for WW and 125 °C for SRC. The total weight
463 losses in the second reaction zone were in the range of 15–33% for all studied fuels; 17% for
464 BS, 22% for MIS, 20% for WW, 33% for WS, 15% for SRC and 20% for WP. The maximum
465 rate of weight loss (wt% /min) 12.6% for SRC was observed in the char combustion zone.
466 These weight loss values (except WS in zone two) were lower than under air which is in
467 contrast with zone one, where weight loss values are slightly higher than under air.
468
469 The thermal degradation results of both reaction zones under the oxy-fuel combustion
470 condition are summarised in Table S2. The comparative analysis of DTG profiles of Fig. 1b
471 and Fig. 3b revealed close proximity of peak temperatures for both devolatilisation and char
472 combustion zones. Thermal degradation analysis under air and oxy-fuel also suggests that by
473 replacing N_2 with CO_2 as the diluent; no unfavourable effect on the thermal degradation of
474 biomass fuels was observed, provided O_2 concentration was increased from 21 to 30%. This
475 has also been confirmed on larger scale study [54] that gas temperature profiles were similar
476 to that of conventional air combustion. The studied biomass fuels burned at relatively reduced
477 temperatures in oxy-fuel as compared to air. The residual left at the end of second reaction zone
478 consists of ash with 6.5, 5, 1, 9, 2 and 0.5% for BS, MIS, WW, WS, SRC and WP respectively.
479 As previously stated, the combustion characteristics and reaction rates decrease by simply
480 replacing N_2 with CO_2 in the air. Higher concentrations of oxygen are required to match these

characteristics under oxy-fuel conditions as compared to air combustion although parity can be obtained by increasing oxygen concentration up to 30% [54].

Char combustion zones of under both air and oxy-fuel environment are mentioned in Table S1 and Table S2 respectively. The values of T_{peak} and R_{max} in this zone under both reactant gas mixture are comparable to some extent but for some biomasses under oxy-fuel shown higher values for both T_{peak} and R_{max}, this could be associated with higher oxygen ratio in this mixture of reactant gas. The T_{peak} for oxy-fuel char combustion of different biomass found in 378–479 ^{o}C range with R_{max} 4.88–12.65 wt%/min (Table S2), while for air char combustion T_{peak} ranges from 387–483^{o}C with 4.78–9.47 wt %/min R_{max} (Table S1). This data indicates that under oxy-fuel a slight higher R_{max} were observed. Oxy-fuel is better/novel technology and used for CO_2 capture.

Thermal degradation analysis of biomass under this mixture (30% O_2/70% CO_2) of oxy-fuel combustion shows equal and somewhat higher properties than air combustion also correlate with the the literature [54]. Under different thermal degradation zones of oxy-fuel combustion, T_{peak} and R_{max} were observed comparable and higher than air. Moreover, 95 % pure CO_2 capture suggests that this technique could become as one of the leading for combustion of biomass in power plants with even negative CO_2 emission characteristics. Among all studied biomasses under oxy-fuel, air combustion the best biomass fuel with higher T_{peak} and R_{max} were observed in this order SRC> BS>MIS and SRC>MIS>BS respectively. The T_{peak} and R_{max} values of BS and MIS differ slightly under air and oxy-fuel that could be because of the similar volatile matter content.

3.6 Reactivity and kinetic analysis

In all DTG profiles except N_2, two combustion or gasification steps may be seen clearly, the peaks differing in position and height. Therefore, information on biomass samples reactivities may be deduced. Thus reactivities parameters were calculated for each peak, adding the share of any secondary peaks or shoulders present in the burning profile. In this way a value representing the mean reactivity (R_M) was calculated with the corresponding peak temperature (T_p) for all biomass samples; the results are presented in Table 3. The reactivity parameters under N_2 focus on the temperature range of 190 to 460 ^oC, where the maximum value is associated with SRC. Under air, CO_2 and oxy-fuel there are additional reactions from devolatilisation, char gasification and combustion. Temperature ranges from 205 to 370 ^oC and 315 to 570 ^oC are associated with volatile combustion zones and char combustion zones under air and oxy-fuel respectively.

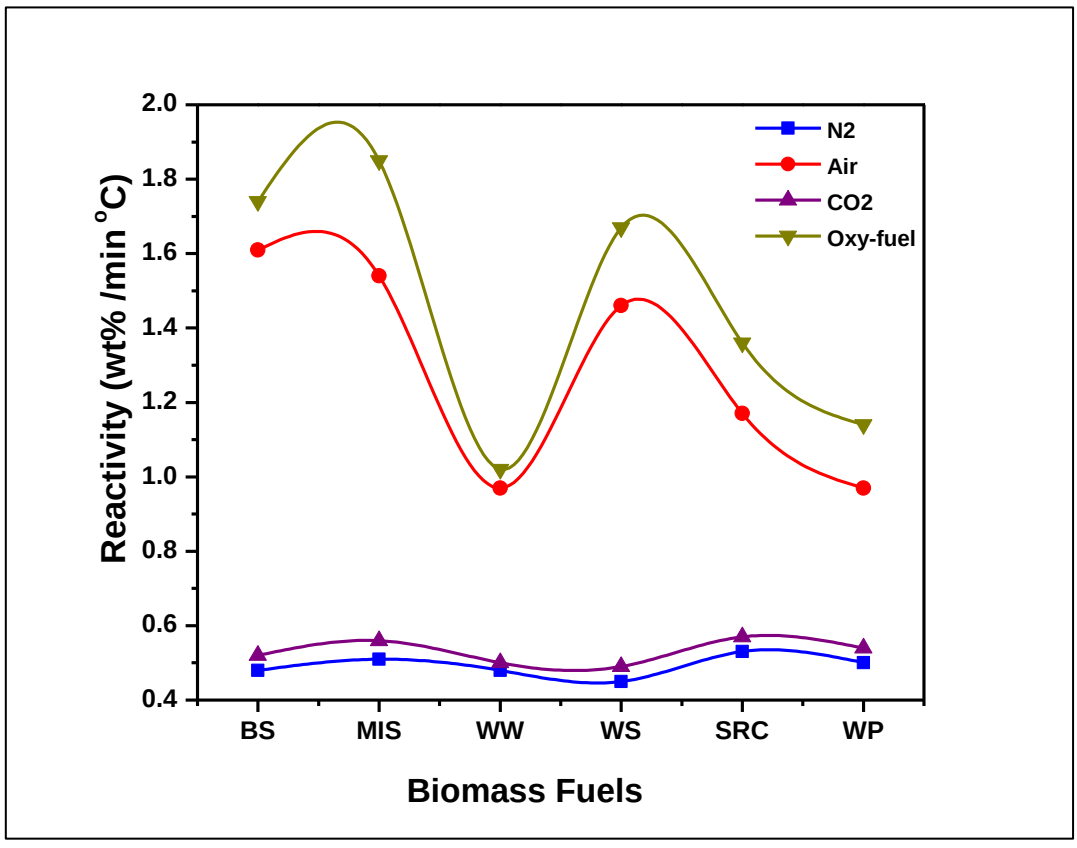

Fig. 6. Reactivity profiles of biomass fuels under different reaction environment.

519 Under oxy-fuel, higher reactivity values were noticed as compared to all other reactive
520 environments. Temperature range from 200 to 415 ^{o}C and 680 to 950 ^{o}C are attributed as
521 devolatilisation and char-CO_2 reaction zones respectively. The biomass fuels such as BS, MIS,
522 and WS with lower lignin content showed higher reactivities.
523
524 For comparative analysis based on the values of R_M the fuel samples may be ranked as
525 SRC>MIS>WP>BS>WW>WS under N_2 and CO_2 , but under CO_2 the R_M values are slightly
526 higher than as under N_2. Similarly these values are greater under oxy-fuel as compared to air
527 and show a trend as MIS>BS>WS>SRC>WP>WW. For air the trend is as
528 BS>MIS>WS>SRC>WP>WW. Under above mentioned conditions different trends were
529 observed but there is a small and comparable difference between their R_M values. As under N_2
530 SRC willow exhibited high R_M value of 0.53, whereas the next fuel with high R_M is MIS (0.51)
531 and this biomass fuel is exhibited high R_M under oxy-fuel combustion reactivity analysis. R_M
532 value of 1.60 is observed for BS under air, while this fuel at the first rank under air and at
533 second rank under oxy-fuel analysis. R_M values under oxy-fuel were observed to be higher than
534 those under air, a phenomenon which is also supported by [59], and one of the reasons this
535 process is valued as an alternative to conventional combustion.

536

537 **Table 3.** Reactivity parameters of biomass fuels under N_2, Air, CO_2 and Oxy-fuel environments.

Fuels (from this study unless stated)	**Under N_2**		**Under Air (21%O_2/79%N_2)**			**Under CO_2**			**Under Oxy-fuel (30%O_2/70%CO_2)**		
	Peak Temp T_p (ºC)	Reactivity $R_M \times 10^2$ (wt% /min ºC)	Peak Temp T_{p1} (ºC)	Peak Temp T_{p2} (ºC)	Reactivity $R_M \times 10^2$ (wt%/ min ºC)	Peak Temp T_{p1} (ºC)	Peak Temp T_{p2} (ºC)	Reactivity $R_M \times 10^2$ (wt%/ min ºC)	Peak Temp T_{p1} (ºC)	Peak Temp T_{p2} (ºC)	Reactivity $R_M \times 10^2$ (wt% /min ºC)
BS	335	0.48	288	401	1.61	336	809	0.52	296	433	1.74
MIS	341	0.51	295	387	1.54	343	912	0.56	299	388	1.85
WW	371	0.48	330	456	0.97	370	909	0.50	335	465	1.02
WS	333	0.45	293	403	1.46	331	938	0.49	285	378	1.67
SRC	367	0.53	338	483	1.17	367	889	0.57	331	479	1.36
WP	376	0.50	346	477	0.97	379	945	0.54	340	474	1.14

538

539

540 Under N_2, CO_2, air and oxy-fuel from pyrolysis to combustion, different reactivities have been
541 observed. The reasons behind differences in the reactivity profile of these biomasses are: (1)
542 physical characteristics, (2) elemental and structural components, (3) moisture content, and (4)
543 char combustion rate. Different char combustion rate might be credited to the varied reaction
544 environment applied to the non-isothermal TGA of the biomasses. Somewhat similar R_M values
545 were noted for biomasses under air and oxy-fuel, might because of O_2 composition of these
546 environments as shown in Fig. 6. As would be expected, an increase in char reactivity with
547 increasing O_2 concentration was also observed for both O_2/N_2 and O_2/CO_2 combustion
548 environments.

549

550 The kinetic parameters of all type of fuels were determined from TGA profiles using a linear
551 form of the Arrhenius equation. The activation energy (Ea), order of reaction (n) and
552 correlation coefficient (R^2) calculated under different atmospheres of the studied biomass fuels.
553 The reaction kinetics were modelled at n = 0.5, n =1 and n =2 and it was found that values of
554 Ea increased by as much as twofold between n = 0.5 and n = 2. The best line of fit for the
555 apparent energy of activation values has been reported for 0.5 order of reaction and is
556 represented in Table 4. There is no consensus in the literature as to reaction order, with some
557 studies supporting these results [33] but others affirming that pyrolysis is best described as a
558 global first order reaction [32]. For comparison of rate constants, Arrhenius plots of all biomass
559 fuels are shown in Fig. 7. In the devolatilisation zone, there were no significant differences
560 among the rate constants of the samples. In the early stages of thermal degradation, the WS
561 had a slightly higher rate constant than those of the other fuels. The BS maintained a high rate
562 constant, whereas the WP maintained a low rate constant until the end of the first zone. The

563 rate constant of the BS reached to its maximum at the end of the first zone under all reaction
564 environments.

565

566 **Table 4.** Kinetic parameters of biomass fuels under N_2, Air, CO_2 and Oxy-fuel environments.

Fuels (from this study unless stated)	**Under N_2**		**Under Air (21%O_2/79%N_2)**				**Under CO_2**				**Under Oxy-fuel (30%O_2/70%CO_2)**			
	Devolatilisation zone n=0.5		Devolatilisation zone n=0.5		Char combustion zone n=0.5		Devolatilisation zone n=0.5		Char CO_2 reaction zone n=0.5		Devolatilisation zone n=0.5		Char combustion zone n=0.5	
	Ea kJ/mole	R^2	Ea kJ/mole	R^2	Ea kJ/mole	R^2	Ea kJ/mole	R^2	Ea kJ/mole	R^2	Ea kJ/mole	R^2	Ea kJ/mole	R^2
BS	84.69	0.96	140.07	0.95	380.16	0.92	82.82	0.98	325.10	0.92	155.18	0.95	194.48	0.93
MIS	92.11	0.97	159.33	0.96	303.78	0.85	80.30	0.99	229.42	0.85	175.73	0.96	226.80	0.99
WW	86.72	0.97	110.88	0.96	197.58	0.83	85.46	0.97	334.71	0.87	111.40	0.97	339.73	0.83
WS	98.68	0.96	160.20	0.94	167.79	0.85	82.65	0.99	305.00	0.91	204.87	0.99	203.82	0.83
SRC	76.95	0.95	103.63	0.96	170.05	0.85	75.20	0.94	543.99	0.87	115.51	0.98	333.01	0.93
WP	81.67	0.97	102.45	0.95	198.85	0.83	80.57	0.96	428.22	0.88	112.52	0.92	417.21	0.94

567

The slopes of Arrhenius plots help in the determination of the levels of activation energies of these biomass fuels. The highest slope compatible with WS with activation energy 96.98 kJ/mole (under N_2), 160.20 kJ/mole (under air) and 204.87 kJ/mole (under oxy-fuel). While the lowest slopes belong to the SRC and WP, both of which have an activation energy of 76.95 kJ/mole (under N_2), 75.20 kJ/mole (under CO_2) and 102.45 kJ/mole (under air) respectively. The apparent activation energy values in devolatilisation zone under N_2 were 98.68>92.11>86.72>84.69>81.67>76.95 for WS>MIS>WW>BS>WP>SRC respectively. Under CO_2 Ea values were observed in the order of WW>BS>WS WP>MIS>SRC and SRC>WP>WW>BS>WS>MIS in devolatilisation zone and char-CO_2 reaction zone respectively. Higher activation energies were observed mostly for soft woody samples whereas for comparatively harder ones lower activation energies were observed.

In the char combustion or gasification zone, much higher rate constants were noticed for the BS under air, SRC under CO_2 and WP under oxy-fuel, when compared to the others. At the beginning of the second zone, the rate constant of the MIS under air was observed higher than that of the BS. Both of these had a closer rate constants as the end of that zone was nearer. Under air BS also had higher slope second zone due to its significantly high activation energy (380.16 kJ/mol) as compared to WS (167.79 kJ/mol). Amid the other six samples, the wheat straws had to some extent higher rate constants in the early phases of the second reaction zone. This turned into even less significant towards the end of this reaction zone. The apparent activation energy values 160.20>159.33>140.07>110.88>103.63>102.45 for WS>MIS>BS>WW>SRC>WP respectively were observed under air in devolatilisation zone. The calculated apparent Ea values under oxy-fuel were as 204.87>175.73>155.18>115.51>112.52>111.40 for WS>MIS>BS>SRC>WP>WW in

592 devolatilisation zone. The above trends of activation energy could be associated with the nature

593 of soft and hardwood residues under different zones.

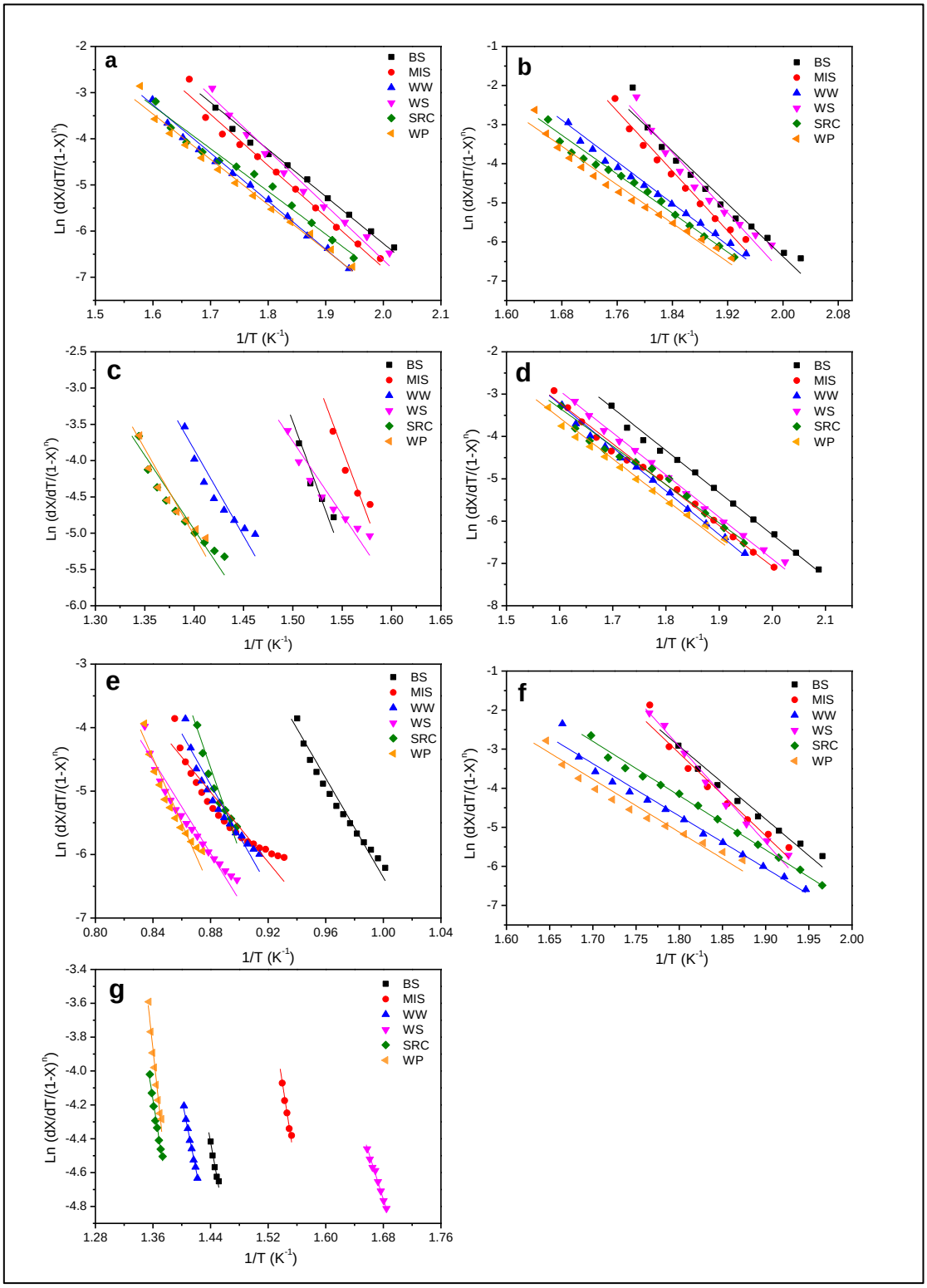

594

595 **Fig. 7.** Arrhenius plots for biomass fuels under: (a) N_2, (b) Air devolatilisation zone, (c) Air char
596 combustion zone, (d) CO_2 devitalisation zone, (e) CO_2 char-CO_2 reaction zone, (f) Oxy-fuel
597 devolatilisation zone and (g) Oxy-fuel char combustion zone.

With an increase in oxygen concentration, the apparent energy barriers decrease resulting in lower values of Ea for both volatile and char combustion zones. However, in the present case, after replacing N_2 with CO_2 under oxy-fuel the apparent barrier towards the volatile and char combustion reaction zone increases resulting in relatively higher values of Ea. This could be partly due to the physical properties of CO_2 in oxy-fuel. The rest of the apparent Ea values found to be nearly synchronised with existing literature [11]. Therefore, Table 4 values are supported and verified from Table 3 values. According to Ea and reactivity profile trend under N_2, the most reactive biomass with the least activation energy is SRC and the least reactive with high activation energy is WS. A significantly similar type of results under other experimental conditions were observed.

Heat flow and mass transfer rates of the biomass fuels were determined under N_2 and air reaction environments. Fig. 8 and Fig. 9 show the experimental DSC thermograms of biomass fuels under N_2 and air respectively. To detect the endothermic and exothermic nature of the reactions heat transfer analyses were performed. From DSC results, it was observed that the thermograms went from endothermic reactions to very minor exothermic ones. The first region of endothermic peaks was noted up to 300 ^oC, then very minor exothermic peaks were observed up to 700 ^oC. The peaks above 300 ^oC can be attributed to the degradation of the lignocellulosic components [2]. After this, the fuels were degraded again in the endothermic region. These thermograms ensured that all biomass fuels were degraded under endothermic region without the effect of self-heating [2]. Fig. 8b shows the mass transfer rates of the fuels under N_2. All fuels show relatively slow (pyrolysis) mass conversion under N_2 than air (combustion) (Fig. 9b), these results are in agreement with [60]. Fig. 9a shows that thermograms went from endothermic to exothermic reactions when the temperature increased above 280 ^oC. Two

exothermic peaks were noted for all type of biomass fuels combustion from 280 to 500 °C, peak 1 was observed due to light volatiles combustion while peak 2 was noticed for fixed carbon combustion [13, 61]. These significant exothermic peaks were considered in accordance with the mass conversion profiles and verified from study [61]. The exothermic peaks were exhibited because of the oxidant environment. After this, the biomass fuels again degraded under the endothermic region.

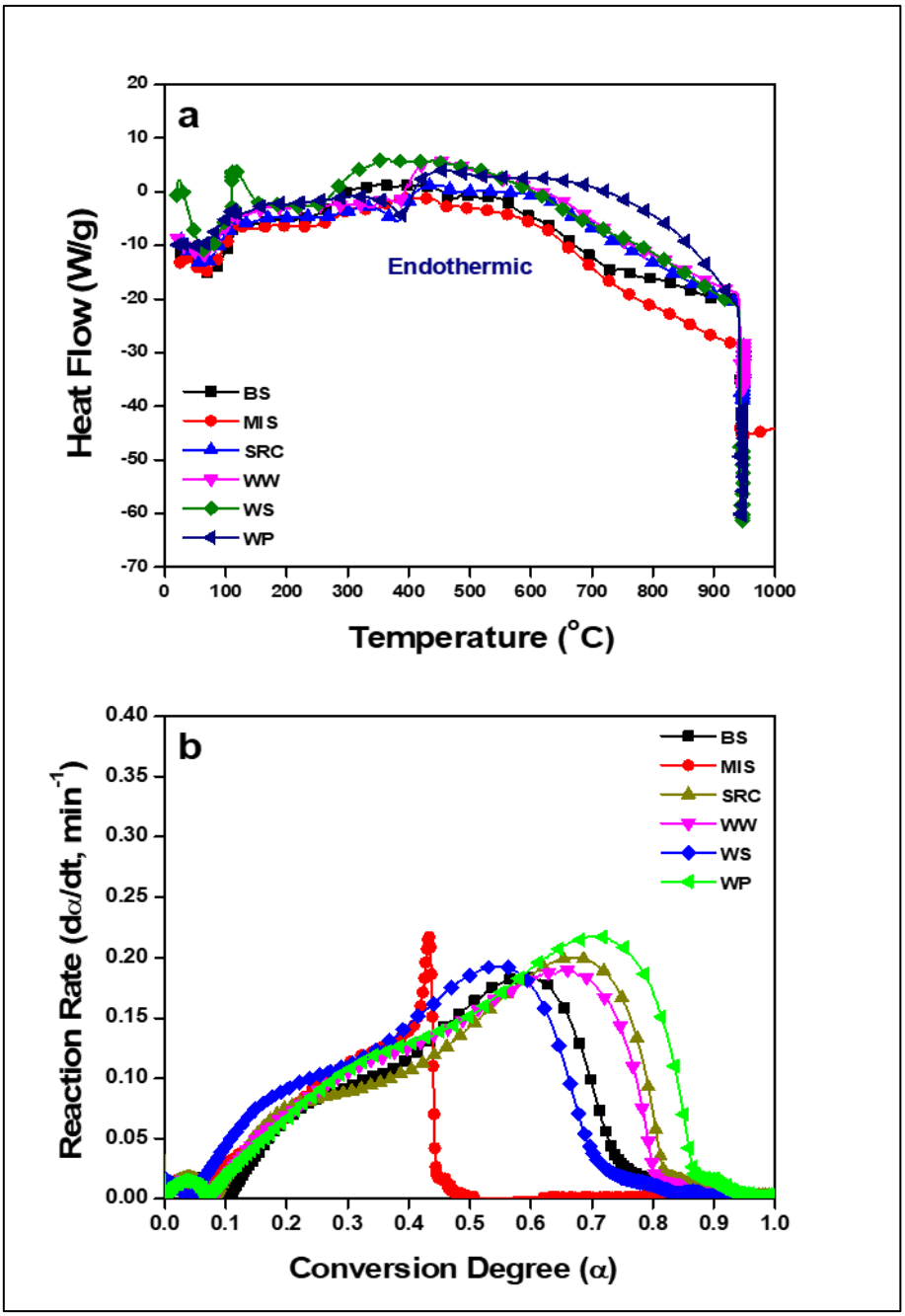

Fig. 8. DSC analysis of biomass fuels under N_2: (a) Heat flow, (b) Mass transfer rates.

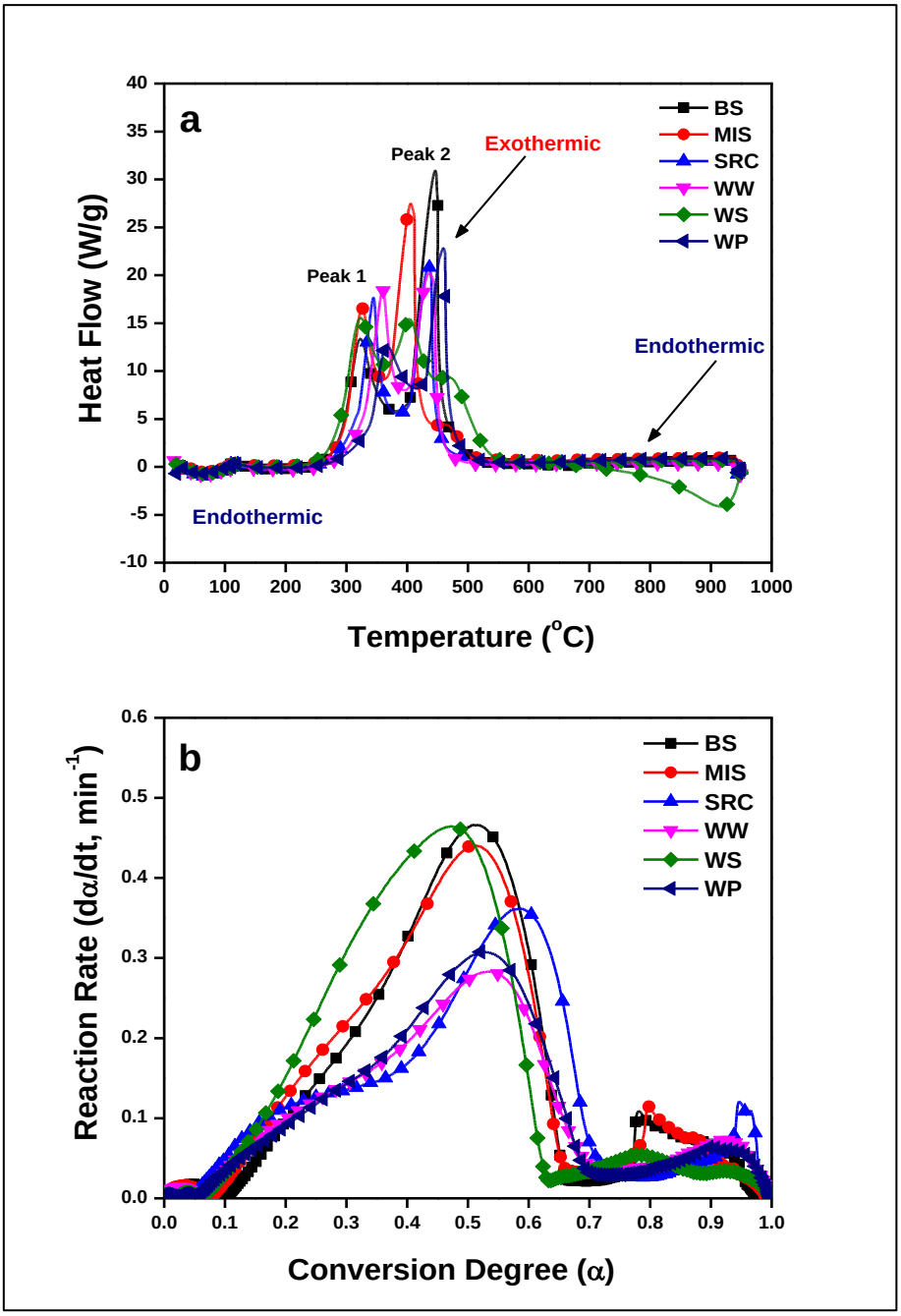

Fig. 9. DSC analysis of biomass fuels under air: (a) Heat flow, (b) Mass transfer rates.

The rate of mass transfer of MIS, WP and SRC were detected higher than other fuels under N_2, while under air the rate of BS, WS and MIS mass transfer was higher than others. The mass

transfer rates of the mentioned fuels were in near agreement with their reactivities under similar reaction environment. It can be observed clearly from the (Fig. 8b and Fig. 9b) that the rate of mass transfer is faster under air than N_2 and was noted like this as of respective DSC heat release curves [35, 60].

4. Conclusions

This study is focused on the assessment of diverse biomass fuels as a renewable energy source for power and energy generation. The investigated biomass fuels include woody (waste wood, wood pellets), non-woody (miscanthus, wheat straw) and special type (short rotation coppicing (SRC willow). Thermogravimetric analyses (TGA) and differential scanning calorimetry (DSC) analyses were performed under four different reaction environments including; N_2, air, CO_2 and the oxy-fuel (30% O_2/70% CO_2). The findings of this work are summarised as follows:

- The carbon content of biomass samples ranges (40.87–47.02%), most of these were comparable (BS, MIS and WS C content), higher (SRC, WW and WP C content) than the reported biomasses (40.93–43.19%) and lignite: low rank coal (44.82%) C content respectively. Wheat straw (WS) contains the highest fixed carbon at 18.22%, whereas, SRC has the highest amount of volatile matter at 85%.
- The rate of thermal decomposition for any type of biomass fuels in an inert atmosphere was slower than in an oxidising atmosphere also confirmed from mass transfer rates.
- Thermal degradation analysis under air and oxy-fuel also suggests that by replacing N_2 with CO_2 as the diluent; no unfavourable effect on thermal degradation of biomass fuels was observed provided oxygen percentage was increased from 21 to 30%.
- In terms of reactivity, under different thermal degradation zones of oxy-fuel combustion, T_{peak} and R_{max} were observed comparable and slightly higher than air. Moreover, 95% pure CO_2 capture suggests that this technique could become the leading

664 one for combustion of biomass in the UK's power plants with negative CO_2 emission
665 characteristics.

666 • The T_{peak} and R_{max} values of BS and MIS differ slightly under air and oxy-fuel might
667 because both have the same volatile matter content.

668 • It is observed that the reactivity (R_M) order in case of N_2 and CO_2 is
669 SRC>MIS>WP>BS>WW>WS. Similarly, R_M order of BS>MIS>WS>SRC>WP>WW
670 is observed under air and oxy-fuel, except the R_M of MIS>BS in oxy-fuel case.

671 • Based on linear regression analysis of half, first and second order, the closest modelled
672 fit occurred with a reaction order of n= 1/2 for all samples and conditions.

673 • Higher activation energies with lower reactivity were observed for the biomass fuels
674 that have low cellulosic contents as compared to the other fuels.

675 • DSC thermograms under N_2 confirmed that all biomass fuels were degraded in the
676 endothermic region without the effect of self-heating, while for air combustion two
677 significant exothermic peaks were noticed.

678 • The most reactive biomass with least activation energy is SRC and the least reactive
679 with high activation energy is WS, somewhat nearly similar results were observed
680 under all experimental conditions.

References

[1] F. Sher, M.A. Pans, D.T. Afilaka, C. Sun, H. Liu. Experimental investigation of woody and non-woody biomass combustion in a bubbling fluidised bed combustor focusing on gaseous emissions and temperature profiles. Energy. 141 (2017) 2069-80.

[2] R.K. Mishra, K. Mohanty. Pyrolysis kinetics and thermal behavior of waste sawdust biomass using thermogravimetric analysis. Bioresource technology. 251 (2018) 63-74.

[3] P. McNamee, L. Darvell, J. Jones, A. Williams. The combustion characteristics of high-heating-rate chars from untreated and torrefied biomass fuels. Biomass and bioenergy. 82 (2015) 63-72.

[4] I.U. Hai, F. Sher, A. Yaqoob, H.J.F. Liu. Assessment of biomass energy potential for SRC willow woodchips in a pilot scale bubbling fluidized bed gasifier. 258 (2019) 116143.

[5] K. Jayaraman, I. Gökalp. Pyrolysis, combustion and gasification characteristics of miscanthus and sewage sludge. Energy Conversion and Management. 89 (2015) 83-91.

[6] E. Forbes, D. Easson, G. Lyons, W. McRoberts. Physico-chemical characteristics of eight different biomass fuels and comparison of combustion and emission results in a small scale multi-fuel boiler. Energy conversion and management. 87 (2014) 1162-9.

[7] I.U. Hai, F. Sher, G. Zarren, H.J.J.o.C.P. Liu. Experimental investigation of tar arresting techniques and their evaluation for product syngas cleaning from bubbling fluidized bed gasifier. 240 (2019) 118239.

[8] Y. Ding, O.A. Ezekoye, S. Lu, C. Wang, R. Zhou. Comparative pyrolysis behaviors and reaction mechanisms of hardwood and softwood. Energy conversion and management. 132 (2017) 102-9.

[9] M. Wilk, A. Magdziarz, K. Jayaraman, M. Szymańska-Chargot, I. Gökalp. Hydrothermal carbonization characteristics of sewage sludge and lignocellulosic biomass. A comparative study. Biomass and Bioenergy. 120 (2019) 166-75.

[10] K. Mansaray, A. Ghaly. Thermal degradation of rice husks in nitrogen atmosphere. Bioresource technology. 65 (1998) 13-20.

[11] S. Munir, S. Daood, W. Nimmo, A. Cunliffe, B. Gibbs. Thermal analysis and devolatilization kinetics of cotton stalk, sugar cane bagasse and shea meal under nitrogen and air atmospheres. Bioresource technology. 100 (2009) 1413-8.

[12] X. Yao, Q. Yu, Z. Han, H. Xie, W. Duan, Q. Qin. Kinetics of CO2 gasification of biomass char in granulated blast furnace slag. International Journal of Hydrogen Energy. 43 (2018) 12002-12.

[13] M. Mureddu, F. Dessì, A. Orsini, F. Ferrara, A. Pettinau. Air-and oxygen-blown characterization of coal and biomass by thermogravimetric analysis. Fuel. 212 (2018) 626-37.

[14] P. Ollero, A. Serrera, R. Arjona, S. Alcantarilla. The CO_2 gasification kinetics of olive residue. Biomass and Bioenergy. 24 (2003) 151-61.

[15] R. Khalil, G. Várhegyi, S. Jäschke, M.G. Grønli, J. Hustad. CO_2 gasification of biomass chars: a kinetic study. Energy & Fuels. 23 (2008) 94-100.

[16] W. Klose, M. Wölki. On the intrinsic reaction rate of biomass char gasification with carbon dioxide and steam. Fuel. 84 (2005) 885-92.

[17] S. Scott, J. Davidson, J. Dennis, P. Fennell, A. Hayhurst. The rate of gasification by CO_2 of chars from waste. Proceedings of the Combustion Institute. 30 (2005) 2151-9.

[18] S.S. Idris, N.A. Rahman, K. Ismail, A.B. Alias, Z.A. Rashid, M.J. Aris. Investigation on thermochemical behaviour of low rank Malaysian coal, oil palm biomass and their blends during pyrolysis via thermogravimetric analysis (TGA). Bioresource technology. 101 (2010) 4584-92.

[19] T. Xu, F. Xu, Z. Hu, Z. Chen, B. Xiao. Non-isothermal kinetics of biomass-pyrolysis-derived-tar (BPDT) thermal decomposition via thermogravimetric analysis. Energy Conversion and Management. 138 (2017) 452-60.
[20] Y. Zhang, Z. Zhang, M. Zhu, F. Cheng, D. Zhang. Interactions of coal gangue and pine sawdust during combustion of their blends studied using differential thermogravimetric analysis. Bioresource technology. 214 (2016) 396-403.
[21] S. Şensöz, D. Angın, S. Yorgun. Influence of particle size on the pyrolysis of rapeseed (Brassica napus L.): fuel properties of bio-oil. Biomass and Bioenergy. 19 (2000) 271-9.
[22] H.H. Sait, A. Hussain, A.A. Salema, F.N. Ani. Pyrolysis and combustion kinetics of date palm biomass using thermogravimetric analysis. Bioresource Technology. 118 (2012) 382-9.
[23] S. Channiwala, P. Parikh. A unified correlation for estimating HHV of solid, liquid and gaseous fuels. Fuel. 81 (2002) 1051-63.
[24] H. Li, S. Xia, P. Ma. Thermogravimetric investigation of the co-combustion between the pyrolysis oil distillation residue and lignite. Bioresource technology. 218 (2016) 615-22.
[25] S.-J. Jung, S.-H. Kim, I.-M. Chung. Comparison of lignin, cellulose, and hemicellulose contents for biofuels utilization among 4 types of lignocellulosic crops. Biomass and Bioenergy. 83 (2015) 322-7.
[26] Y.-J. Xia, H.-Q. Xue, H.-Y. Wang, Z.-P. Li, C.-H. Fang. Kinetics of isothermal and non-isothermal pyrolysis of oil shale. Oil Shale. 28 (2011) 415-24.
[27] H. Liu. Combustion of coal chars in O_2/CO_2 and O_2/N_2 mixtures: a comparative study with non-isothermal thermogravimetric analyzer (TGA) tests. Energy & Fuels. 23 (2009) 4278-85.
[28] X. Zeng, S. Zheng, H. Zhou, Q. Fang, C. Lou. Char burnout characteristics of five coals below and above ash flow temperature: TG, SEM, and EDS analysis. Applied Thermal Engineering. 103 (2016) 1156-63.
[29] R.A. dos Reis Ferreira, C. da Silva Meireles, R.M.N. Assunção, R.R. Soares. Heat required and kinetics of sugarcane straw pyrolysis by TG and DSC analysis in different atmospheres. Journal of Thermal Analysis and Calorimetry. 132 (2018) 1535-44.
[30] Z. Cai, X. Ma, S. Fang, Z. Yu, Y. Lin. Thermogravimetric analysis of the co-combustion of eucalyptus residues and paper mill sludge. Applied Thermal Engineering. 106 (2016) 938-43.
[31] N.S. Yuzbasi, N. Selçuk. Air and oxy-fuel combustion characteristics of biomass/lignite blends in TGA-FTIR. Fuel Processing Technology. 92 (2011) 1101-8.
[32] A. Saddawi, J. Jones, A. Williams, M. Wojtowicz. Kinetics of the thermal decomposition of biomass. Energy & Fuels. 24 (2009) 1274-82.
[33] C.J. Gomez, G. Varhegyi, L. Puigjaner. Slow pyrolysis of woody residues and an herbaceous biomass crop: a kinetic study. Industrial & engineering chemistry research. 44 (2005) 6650-60.
[34] P. Ghetti, L. Ricca, L. Angelini. Thermal analysis of biomass and corresponding pyrolysis products. Fuel. 75 (1996) 565-73.
[35] D. Pottmaier, M. Costa, A. Oliveira, C. Snape. The profiles of mass and heat transfer during pinewood conversion. Energy Procedia. 66 (2015) 285-8.
[36] S. Huang, S. Wu, Y. Wu, J. Gao. The Physicochemical Properties and Catalytic Characteristics of Different Biomass Ashes. Energy Sources, Part A: Recovery, Utilization, and Environmental Effects. 36 (2014) 402-10.
[37] T.R. Miles, T. Miles Jr, L. Baxter, R. Bryers, B. Jenkins, L. Oden. Alkali deposits found in biomass power plants: A preliminary investigation of their extent and nature. Volume 1. National Renewable Energy Lab., Golden, CO (United States); Miles (Thomas R.), Portland, OR (United States); Sandia National Labs., Livermore, CA (United States); Foster Wheeler Development Corp., Livingston, NJ (United States); California Univ., Davis, CA (United States); Bureau of Mines, Albany, OR (United States). Albany Research Center1995.

[38] S.V. Vassilev, D. Baxter, L.K. Andersen, C.G. Vassileva. An overview of the chemical composition of biomass. Fuel. 89 (2010) 913-33.
[39] X. Zhang, M. Xu, R. Sun, L. Sun. Study on biomass pyrolysis kinetics. Journal of engineering for gas turbines and power. 128 (2006) 493-6.
[40] A. Gani, I. Naruse. Effect of cellulose and lignin content on pyrolysis and combustion characteristics for several types of biomass. Renewable Energy. 32 (2007) 649-61.
[41] E. Biagini, F. Barontini, L. Tognotti. Devolatilization of biomass fuels and biomass components studied by TG/FTIR technique. Industrial & engineering chemistry research. 45 (2006) 4486-93.
[42] M. Carrier, A. Loppinet-Serani, D. Denux, J.-M. Lasnier, F. Ham-Pichavant, F. Cansell, et al. Thermogravimetric analysis as a new method to determine the lignocellulosic composition of biomass. Biomass and Bioenergy. 35 (2011) 298-307.
[43] Y.Y. Tye, K.T. Lee, W.N.W. Abdullah, C.P. Leh. The world availability of non-wood lignocellulosic biomass for the production of cellulosic ethanol and potential pretreatments for the enhancement of enzymatic saccharification. Renewable and Sustainable Energy Reviews. 60 (2016) 155-72.
[44] T. Bridgeman, J. Jones, I. Shield, P. Williams. Torrefaction of reed canary grass, wheat straw and willow to enhance solid fuel qualities and combustion properties. Fuel. 87 (2008) 844-56.
[45] H.S. Kambo, A. Dutta. Comparative evaluation of torrefaction and hydrothermal carbonization of lignocellulosic biomass for the production of solid biofuel. Energy conversion and management. 105 (2015) 746-55.
[46] E.M. Hodgson, D. Nowakowski, I. Shield, A. Riche, A.V. Bridgwater, J.C. Clifton-Brown, et al. Variation in Miscanthus chemical composition and implications for conversion by pyrolysis and thermo-chemical bio-refining for fuels and chemicals. Bioresource technology. 102 (2011) 3411-8.
[47] E. Hodgson, R. Fahmi, N. Yates, T. Barraclough, I. Shield, G. Allison, et al. Miscanthus as a feedstock for fast-pyrolysis: Does agronomic treatment affect quality? Bioresource technology. 101 (2010) 6185-91.
[48] R.A. Hague. Pre-treatment and pyrolysis of biomass for the production of liquids for fuels and speciality chemicals. Aston University1998.
[49] C. Greenhalf, D. Nowakowski, A. Harms, J. Titiloye, A. Bridgwater. A comparative study of straw, perennial grasses and hardwoods in terms of fast pyrolysis products. Fuel. 108 (2013) 216-30.
[50] P. McKendry. Energy production from biomass (part 1): overview of biomass. Bioresource technology. 83 (2002) 37-46.
[51] C. Gurgel Veras, J. Saastamoinen, J. Carvalho Jr, M. Aho. Overlapping of the devolatilization and char combustion stages in the burning of coal particles. Combustion and Flame. 116 (1999) 567-79.
[52] D. Dayton, B. Jenkins, S. Turn, R. Bakker, R. Williams, D. Belle-Oudry, et al. Release of inorganic constituents from leached biomass during thermal conversion. Energy & Fuels. 13 (1999) 860-70.
[53] A.G. Borrego, D. Alvarez. Comparison of chars obtained under oxy-fuel and conventional pulverized coal combustion atmospheres. Energy & Fuels. 21 (2007) 3171-9.
[54] H. Liu, R. Zailani, B.M. Gibbs. Comparisons of pulverized coal combustion in air and in mixtures of O_2/CO_2. Fuel. 84 (2005) 833-40.
[55] P.A. Bejarano, Y.A. Levendis. Single-coal-particle combustion in O_2/N_2 and O_2/CO_2 environments. Combustion and flame. 153 (2008) 270-87.
[56] J. Moon, J. Lee, U. Lee, J. Hwang. Transient behavior of devolatilization and char reaction during steam gasification of biomass. Bioresource technology. 133 (2013) 429-36.

828 [57] F. Sher, M.A. Pans, C. Sun, C. Snape, H. Liu. Oxy-fuel combustion study of biomass fuels
829 in a 20 kW th fluidized bed combustor. Fuel. 215 (2018) 778-86.
830 [58] A. Ghaly, A. Al-Taweel. Thermal degradation of cereal straws in air. Energy sources. 12
831 (1990) 439-49.
832 [59] R.K. Rathnam, L.K. Elliott, T.F. Wall, Y. Liu, B. Moghtaderi. Differences in reactivity of
833 pulverised coal in air (O_2/N_2) and oxy-fuel (O_2/CO_2) conditions. Fuel Processing Technology.
834 90 (2009) 797-802.
835 [60] D. Pottmaier, M.r. Costa, T. Farrow, A.A. Oliveira, O. Alarcon, C. Snape. Comparison of
836 rice husk and wheat straw: from slow and fast pyrolysis to char combustion. Energy & Fuels.
837 27 (2013) 7115-25.
838 [61] B. Li, G. Chen, H. Zhang, C. Sheng. Development of non-isothermal TGA–DSC for
839 kinetics analysis of low temperature coal oxidation prior to ignition. Fuel. 118 (2014) 385-91.
840